

Substrate-determined exchange interactions between an STM tip and an adatomKun Tao,^{1,2} Yinye Yu,¹ Wenxuan Zhang,¹ Chenglong Jia,¹ Desheng Xue,¹ and V. S. Stepanyuk²¹Key Lab for Magnetism and Magnetic Materials of Ministry of Education, Lanzhou University, China²Max-Planck-Institute of Microstructure Physics, Halle, Germany

(Received 22 March 2018; revised manuscript received 10 May 2018; published 12 June 2018)

By performing *ab initio* calculations, we reveal an unexpected behavior of the exchange interactions between the Fe STM tip and the Fe adatom on Cu(001) and on a Cu₂N monolayer on Cu(001) surfaces [denoted as Cu₂N/Cu(001)]. A tip-adatom distance-dependent antiferromagnetic-ferromagnetic transition and antiferromagnetic exchange interactions between the tip and the adatom are found for these two junctions, respectively. We demonstrate that the different exchange interactions in these systems are determined by the competition between the tip-adatom and the adatom-substrate interactions. Based on transport calculations, we found that the spin polarization and magnetoresistance in the junction on the Cu(001) system and on the Cu₂N/Cu(001) system depend on the tip-adatom distance.

DOI: [10.1103/PhysRevB.97.224411](https://doi.org/10.1103/PhysRevB.97.224411)**I. INTRODUCTION**

Exchange interactions arise from direct overlap of wave functions or indirect interactions such as superexchange and Ruderman-Kittel-Kasuya-Yosida interactions [1–6], and they play vital roles in determining the magnetic properties of nanostructures. Exchange interactions between magnetic adatoms on substrates are sensitive to their local environments. By introducing neighboring adatoms, spin states [7,8], magnetic anisotropy [9–11], and the Kondo effect [12–16] of magnetic adatoms can be controlled because of modified exchange interactions between them. Moreover, due to the interactions between the adatom and the substrate, the electronic properties of the substrates have significant influence on the magnetic ordering in monolayers [17], in atomic chains [18–20], and on the exchange interactions of impurities [21] and supported dimers [22]. However, due to discrete distances on lattices, measuring the exchange interactions between magnetic adatoms on substrates gives no access to all possible separations.

Equipped with a magnetic tip, the exchange forces [23–25] and interactions [26,27] between the scanning tunneling microscopy (STM) tip and the magnetic sample can be measured and also tuned by varying the tip-substrate distances. Based on experimental and theoretical studies, it was reported that spin states [19,26,27], the Kondo effect [28–33], and magnetic anisotropy [34,35] of nanostructures can be manipulated by tuning the interactions between the tip and the adatom. Most of these investigations paid attention to the interactions between the tip and the adatom; however, the effect of adatom-substrate interactions, i.e., the substrate effect, on the tip-adatom coupling has not been investigated yet. Comprehensive studies are therefore needed to understand the substrate effect on the interactions between the tip and the adatom.

In this paper, we address this issue by performing comprehensive *ab initio* studies which clearly show that the exchange interactions between a magnetic STM tip and a magnetic adatom are strongly affected by adatom-substrate interactions. As an example, we choose the Cu(001) and the Cu₂N/Cu(001)

substrates as typical models. We focused particular attention on the magnetic coupling between the Fe tip and the Fe adatom on these surfaces. The possibility of tuning the coupling in the tip-adatom junction via a sensible choice of the tip-substrate separation is demonstrated. An antiferromagnetic-ferromagnetic transition and antiferromagnetic exchange interactions were found in the junctions on the Cu(001) and Cu₂N/Cu(001) surfaces, respectively. We reveal that the substrate effect on the coupling is caused by the hybridization of electronic states between the adatom and the substrate, which depends on the tip-substrate distance.

II. CALCULATION METHODS

Our calculations were performed within the framework of density functional theory (DFT) as implemented in the Vienna Ab initio Simulation Package (VASP) [36,37] with the projector augmented-wave potentials and the generalized gradient approximation (GGA) developed by Perdew, Burke, and Ernzerhof. The basis set contained plane waves with a kinetic energy cutoff of 520 eV, and the total energy was converged to 10⁻⁷ eV. The GGA+*U* method [38] with different effective *U* values has also been applied to the Cu₂N/Cu(001) system, and the main results remain unchanged [39]. All geometries were optimized without any symmetry constraint until all residual forces on each atom were less than 0.01 eV/Å.

A 3 × 3 supercell (10.91 × 10.91 Å²) was employed in all calculations, and a vacuum layer of about 15 Å, perpendicular to the surface slab, was used to avoid interactions with neighboring supercells. The Cu(001) system consists of five bare Cu(001) layers which contain 18 Cu atoms per layer, with an additional c(2 × 2)N-Cu(100) molecular network (that is, the Cu₂N monolayer) on one side for the Cu(001) case [denoted as Cu₂N/Cu(001)]. The Fe atom is located at the hollow site of the Cu(001) system [40], and it resides on top of the Cu site of the Cu₂N/Cu(001) one, forming covalent bonds with the two neighboring N atoms [35,41–47]. To calculate the exchange interaction between the Fe STM tip and the Fe adatom on the

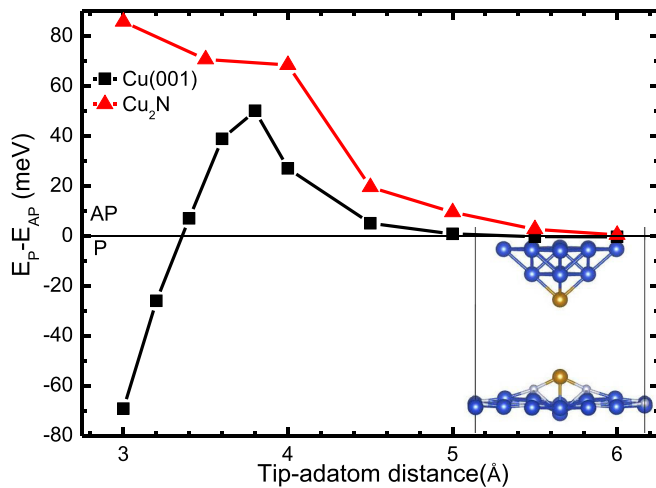


FIG. 1. Exchange energy as a function of the tip-adatom separation for Cu(001) and Cu₂N/Cu(001). The inset is the setup for our calculations.

surfaces, we used a pyramidal cluster model for the STM tip [48], which contains nine Cu atoms and one Fe atom as the apex of the tip. Such a tip can be obtained in experiments by attaching atoms to the tip apex. We have used this model in our previous studies [27,35].

The transmission calculations were performed with the NANODCAL code [49], which combines the DFT with nonequilibrium Green's function formalism. In transmission calculations, we used a double- ζ polarized basis set for all atoms and 10×10 in-plane k points.

III. RESULTS AND DISCUSSION

Figure 1 represents the changes in the exchange energy when the Fe tip is vertically displaced towards the Fe adatom on the Cu(001) or Cu₂N/Cu(001) surface. Here, the exchange energy is defined as $E_{\text{ex}} = E_P - E_{\text{AP}}$, where E_P (E_{AP}) is the total energy of the system with the spin direction of the tip and the adatom in parallel (antiparallel) alignment, denoted as the P (AP) configuration. It was reported by STM experiments that the spin direction of a single Fe adatom [41] or the Fe atomic chain [19] on the Cu₂N/Cu(001) surface is in plane. As pointed out in our previous publication [35], however, when the Fe tip is positioned less than 5 Å above the Fe chain on the Cu₂N/Cu(001) surface, the spin direction of the tip and the chain is out of plane and in a collinear alignment. Therefore, in this paper, we consider only collinear spin alignment calculations. The spin direction of the tip apex is fixed to be spin up, while that of the adatom can be flipped from spin up (P configuration) to spin down (AP configuration) [50]. In low-temperature STM experiments, the spin direction of the tip can be stabilized with an external magnetic field [51]. We focus on the transition between the P and AP configurations. For the Cu(001) surface, the tip-adatom distance-dependent exchange energy shows an antiferromagnetic-ferromagnetic transition. It goes from around zero at large tip-adatom distances to its maximum positive value at 3.8 Å (AP configuration) and then comes to negative values at a tip-adatom distance of 3 Å (P configuration). For the Cu₂N/Cu(001) surface, on the contrary,

only the AP spin configuration between the Fe tip and the Fe adatom was found, with the exchange energy increasing with decreasing tip-adatom distance.

Two interactions exist in these systems, namely, (i) the interaction between the Fe tip and the Fe adatom, and (ii) the substrate effect, or the interaction between the Fe adatom and the Cu(001) or Cu₂N/Cu(001) substrate. The present results suggest that the substrate has an important effect on the interaction between the tip and the adatom. Figure 2(a) shows the lm -decomposed density of states (DOS) projected on the single Fe adatom on the Cu(001) surface, without the tip. The spin-down $d_{x^2-y^2}$ orbital of the Fe adatom is nearly half occupied, while other spin-down d orbitals are nearly empty. Moreover, the d_{xz} and d_{yz} orbitals are degenerated.

As the Fe tip approaches the substrate, it interacts with the Fe adatom on the Cu(001) surface. In order to reveal the physics behind the substrate effect on the exchange coupling between the tip and the adatom, the projected density of states (PDOS) of the Fe adatom on the Cu(001) surface is plotted in Fig. 2. At a tip-adatom distance of 3 Å (P configuration), the direct interaction between them greatly increases due to the strong overlapping of their wave functions, and it is mainly determined by d_{xz} , d_{yz} , and d_{z^2} orbitals. Only the out-of-plane orbitals (d_{xz} , d_{yz} , and d_{z^2}) of the adatom for the P and AP configurations are plotted in the right panel of Fig. 2. For easy comparison with those in the P configuration, the majority and minority parts of the Fe adatom in the AP configuration [Fig. 2(b)] are turned upside down [50]. From Fig. 2(b) it can be observed that, in the AP configuration, the spin-down d_{xz} and d_{z^2} orbitals of the Fe adatom appear just above the Fermi level E_F , and they exhibit a single-atom-like peak. However, the PDOS of the spin-down d_{xz} (d_{z^2}) orbital of the Fe adatom in the P configuration in Fig. 2(c) splits into bonding-antibonding states localized at -0.5 and $+0.24$ eV (-0.48 and $+0.52$ eV), respectively. Similar changes in PDOS can also be found for the Fe tip. The bonding state is more tightly bound, while the antibonding state is energetically destabilized. This corresponds to the Alexander-Anderson model [52,53], which predicts a bonding-antibonding state splitting for a ferromagnetic dimer. Moreover, compared with the AP configuration, the d_{xz} (d_{z^2}) orbital in the P configuration moves to even lower energy, which decreases the total energy of the system and makes the P configuration energetically more favorable.

Increasing the tip-adatom separation to 4 Å, compared to Fig. 2(a), we find that the spin-up $d_{x^2-y^2}$ orbital of the Fe adatom is still half filled but slightly shifted towards the Fermi level [Fig. 3(a)], while the spin-down d_{xz} or d_{yz} orbitals of the Fe tip are half filled [Fig. 3(b)]. For such a separation, the direct interaction between the tip and the adatom is weak. The in-plane $d_{x^2-y^2}$ orbital of the Fe adatom first hybridizes with its own spherically symmetrical s orbital (Fig. 3, left panel) and then interacts with the p_x (p_y) orbitals of the Fe tip, which hybridize with its own d_{xz} (d_{yz}) orbital (Fig. 3, right panel). This superexchange-like interaction is mediated by the sp electrons of the tip and the adatom. Herein electron tunneling between them will play a significant role. As electrons from the half-occupied d_{xz} orbital of the Fe tip, which hybridizes with its p_x orbital, interact with the half-occupied $d_{x^2-y^2}$ orbital of the Fe adatom via its s orbital, they will tend to

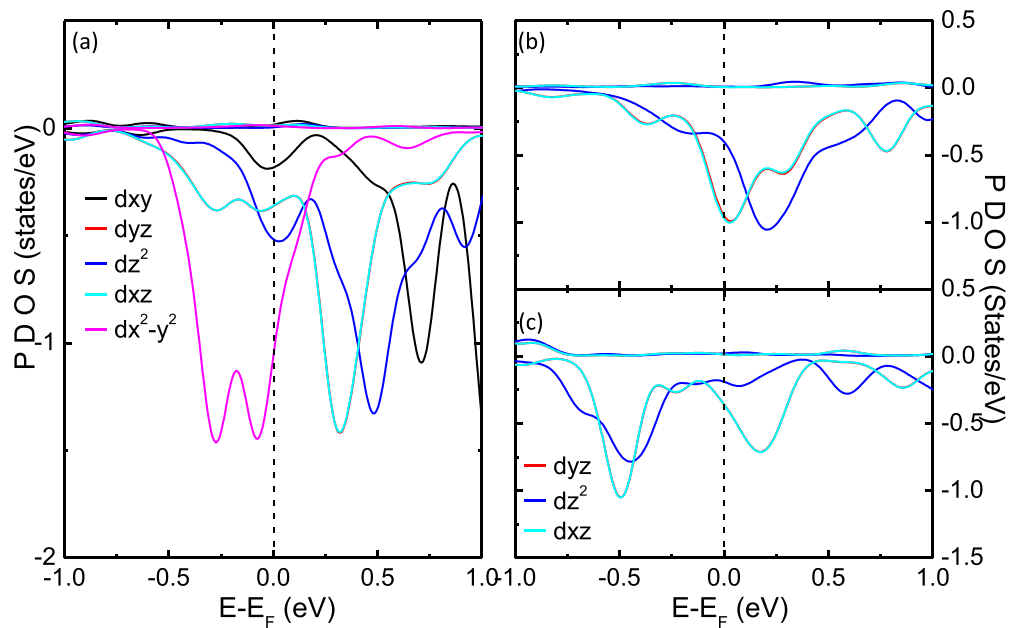


FIG. 2. Projected d -orbital density of states (PDOS) for the Cu(001) system. (a) PDOS for the Fe adatom without the tip. PDOS for the Fe adatom at a tip-adatom separation of 3 Å in (b) the AP configuration and (c) the P configuration.

align their spins antiparallel to lower the total energy of the system, as predicted by Goodenough-Kanamori rules [54–56] (superexchange interaction is antiferromagnetic if the electron transfer occurs between half-filled orbitals). Therefore, the interaction between the Fe tip and the Fe adatom on the Cu(001) surface is based on an antiferromagnetic coupling for this tip-adatom separation.

For the Fe adatom on the Cu₂N/Cu(001) surface, in contrast to that of the Cu(001) surface [Fig. 2(a)], the spin-down $d_{x^2-y^2}$

orbital of the Fe adatom on the Cu₂N/Cu(001) surface is fully occupied, and the d_{z^2} orbital is half occupied [Fig. 4(a)]. This is due to a strong hybridization between the d states of the Fe adatom and the p states of two neighboring N atoms. The degeneracy of d_{xz} and d_{yz} orbitals of the Fe adatom is removed, especially for the spin-up d_{yz} orbital, which appears just above the Fermi level. Moreover, the two neighboring N atoms of the Fe atom have an induced magnetic moment of $0.1\mu_B$, which is much larger than that of $0.03\mu_B$

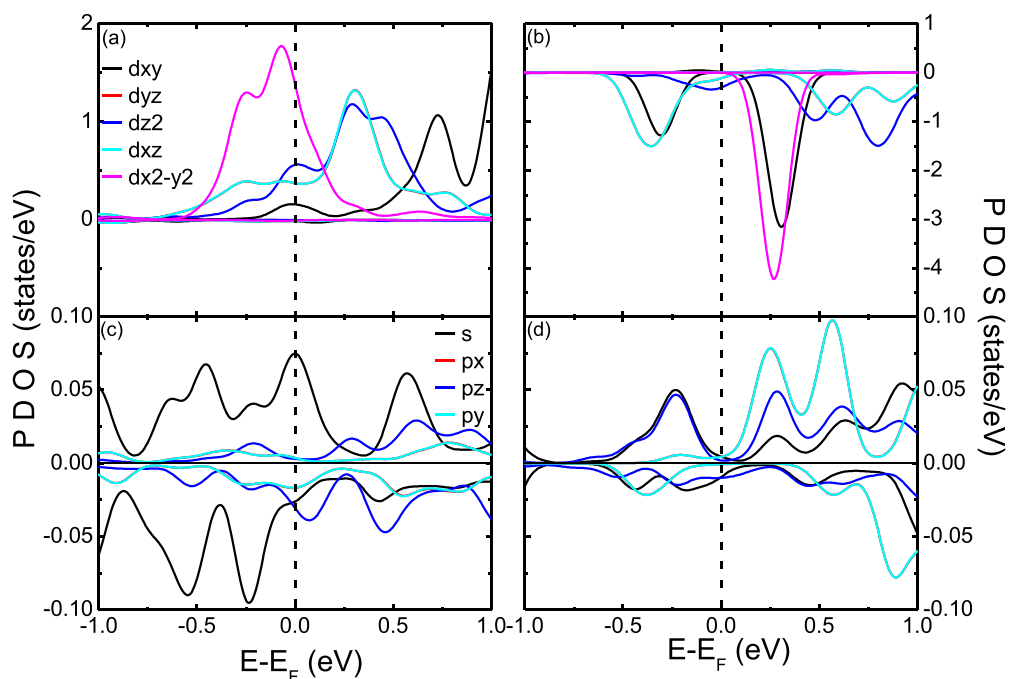


FIG. 3. PDOS for the Cu(001) system at the tip-adatom separation of 4 Å in the AP configuration. Left: (a) d states and (c) sp states of the Fe adatom. Right: (b) d states and (d) sp states of the Fe tip.

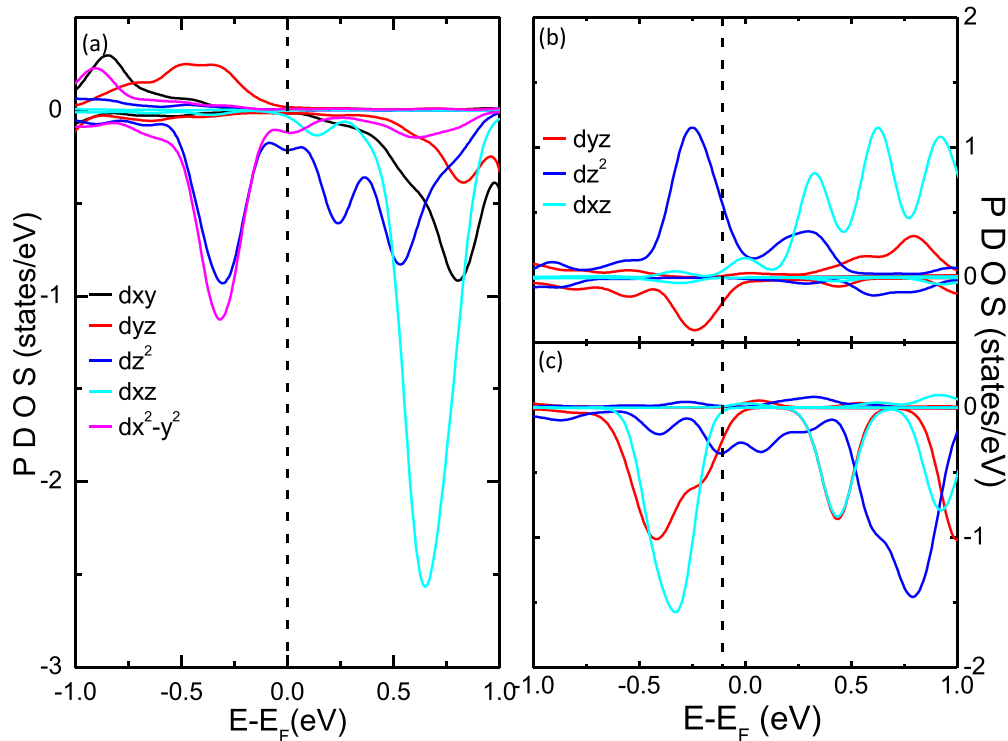


FIG. 4. PDOS for the $\text{Cu}_2\text{N}/\text{Cu}(001)$ system. (a) PDOS for the Fe adatom without the STM tip. PDOS for (b) the Fe adatom and (c) the Fe tip apex at a tip-adatom separation of 3 \AA in the AP configurations.

for Cu atoms around the Fe atom in the $\text{Cu}(001)$ system. Since the Fe atom is embedded in the molecular network of the $\text{Cu}_2\text{N}/\text{Cu}(001)$ surface, the Alexander-Anderson model [52,53], which describes the interaction of two magnetic atoms on neighboring sites in a free-electron-like host metal, is not applicable for the $\text{Cu}_2\text{N}/\text{Cu}(001)$ system.

At larger tip-adatom separations, similar to that for the $\text{Cu}(001)$ system, superexchange-like interactions between the tip and the adatom through $sp-d$ hybridization can also be observed in the $\text{Cu}_2\text{N}/\text{Cu}(001)$ system (not shown), which result in the effective AP configurations. Given that the in-plane spin-up $d_{x^2-y^2}$ orbital of the Fe adatom is nearly unchanged even at short tip-adatom separations, the contributions to the electron transfer through the $d_{x^2-y^2}$ orbital can be safely neglected. The negligible contribution of the $d_{x^2-y^2}$ orbital to the tunneling current in a biased system has been reported for the $\text{Fe}(110)$ surface combined with the Fe tip [57]. The d_{z^2} and d_{yz} orbitals of the Fe atoms are the key player in the arrangement of the spin configuration between the tip and the adatom. Here, we present only the PDOS for out-of-plane orbitals of the Fe tip and the Fe adatom at a tip-adatom distance of 3 \AA [Figs. 4(b) and 4(c)]. One can find that the d_{z^2} orbitals near the Fermi level are mostly involved in the tip-adatom electron transfer. The spin-up d_{z^2} orbital of the Fe adatom shifts to the lower energy and enhances its occupancy to nearly fully filled due to the strong coupling with the Fe tip. The electron transfer from the fully occupied spin-up d_{z^2} orbital of the adatom to empty orbitals of the Fe tip near the Fermi level tends to align their spins antiparallel, lowering the total energy of the system. On the other hand, the fully occupied spin-down d_{yz} orbital of the Fe adatom moves up towards the Fermi level,

and its intensity increases with decreasing tip-adatom distance. Additionally, it hybridizes with the half-occupied spin-down d_{yz} (d_{xz}) orbitals of the Fe tip. The exchange interaction due to the electron transfer from the fully occupied spin-down d_{yz} of the adatom to the half-occupied d_{yz} (d_{xz}) orbitals of the tip starts to increase and gives rise to a ferromagnetic configuration. However, after taking a close look at the electron transfer, as shown in Fig. 5(a), it can be found that the spin-up transmission coefficient is larger than that of the spin-down part. This means that the electron transfer probability for spin-up states from the tip to the adatom is larger than that for spin-down states. As above, the former case results in an antiferromagnetic coupling between the tip and the adatom, while the latter case favors a ferromagnetic coupling. Thus, an effective AP spin configuration between the tip and the adatom is more energetically preferable, as shown in Fig. 1.

We now analyze the substrate effect on the electron transfer for two systems. The zero-bias transmission coefficients between the Fe tip and the Fe adatom on the $\text{Cu}(001)$ and $\text{Cu}_2\text{N}/\text{Cu}(001)$ surfaces at a tip-adatom distance of 3 \AA (4 \AA) in the P and AP spin configurations are presented in Fig. 5. At a tip-adatom separation of 3 \AA , for the $\text{Cu}(001)$ system, the P configuration is the ground state, while the AP configuration has a lower energy for the $\text{Cu}_2\text{N}/\text{Cu}(001)$ system. At first glance, it can be seen that for all spin configurations the transmission coefficients of the $\text{Cu}(001)$ system are larger than those of the $\text{Cu}_2\text{N}/\text{Cu}(001)$ system. In the former case, electrons hop from the Fe tip to the Fe adatom on the metallic surface, while for the latter case electrons hop from the Fe tip to the Fe adatom, which forms covalent bonds with the N atoms on the $\text{Cu}_2\text{N}/\text{Cu}(001)$ surface. Therefore, electrons

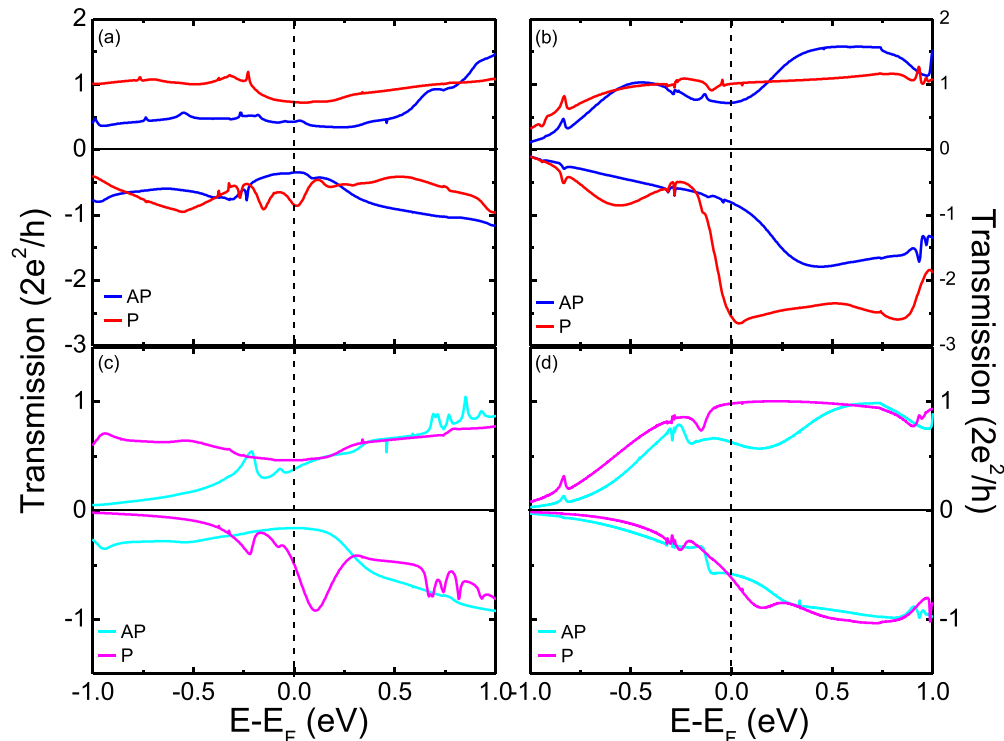


FIG. 5. Zero-bias transmission coefficients for the junction on the $\text{Cu}_2\text{N}/\text{Cu}(001)$ system (left panel) for the P and AP alignments at a tip-adatom distance of (a) 3 Å and (b) 4 Å and those on the $\text{Cu}(001)$ system (right panel) for the P and AP alignments at a tip-adatom distance of (c) 3 Å and (d) 4 Å.

in the junction on the $\text{Cu}(001)$ system have a larger transfer probability than those on the $\text{Cu}_2\text{N}/\text{Cu}(001)$ system.

For the P configuration in the $\text{Cu}(001)$ system [Fig. 5(b)], the spin-up transmission at the Fermi level E_F is around 1, which shows that only one channel contributes to the transmission. This can be further confirmed from Fig. 5(d), which shows that the spin-up transmission at the Fermi level is nearly unchanged with an increased tip-adatom distance of 4 Å. One can clearly relate various peaks in the transmission with peaks in the PDOS of Fig. 2. The spin-down transmission at E_F is in the range of 2 to 3 and significantly larger than the one for spin-up spins, which means that more than one channel is involved in the electron transfer. This is due to the fact that for the spin-down part, there are significant contributions to the PDOS from s and d electrons. For spin-up electrons, the contribution from d electrons is very small, and the only possible channel is the s channel. Therefore, a large spin polarization can be expected. The spin polarization ratio is defined as $P = (T_\uparrow - T_\downarrow)/(T_\uparrow + T_\downarrow)$, where T_\uparrow (T_\downarrow) are the transmission coefficients for all spin-up (spin-down) states at E_F . In contrast to the positive spin polarization for single Fe atoms on the $\text{Cu}(001)$ surface [58], it can be observed from Fig. 5(b) that a large negative spin polarization, $P = -43\%$, is obtained. This can be related to the strong hybridization of d states between the tip and the adatom at the Fermi level (see Fig. 2). Moreover, the spin polarization changes sign at 0.25 eV below the Fermi level. The negative spin polarization may be achieved under finite bias voltage; however, that is beyond the scope of this paper. When the tip-adatom distance increases to 4 Å [Fig. 5(d); the ground state is the AP configuration], however, only a smaller

positive spin polarization, $P = +4\%$, is observed with strongly reduced contributions from spin-down states. This is because the sp states show strong dispersion character and decay slowly in the vacuum, while the d states are more localized and decay fast in the vacuum. As for the AP configuration of the $\text{Cu}_2\text{N}/\text{Cu}(001)$ system with 3 Å [Fig. 5(a)], the spin-up transmission coefficient at E_F is slightly larger than that of spin down, resulting in a smaller positive spin polarization, $P = +10\%$. As the tip-adatom distance increases to 4 Å [Fig. 5(c); AP configuration], the transmission coefficient for spin-up states at E_F is nearly unchanged, while that for the spin-down states is significantly reduced, and a larger spin polarization, $P = +40\%$, is observed. This analysis further supports the conclusion that for the Cu_2N system the transfer probability for spin-up electrons is larger than that for the spin-down electrons.

The transmission coefficients for the AP configuration of the $\text{Cu}(001)$ system and the P configuration of the $\text{Cu}_2\text{N}/\text{Cu}(001)$ system at a tip-adatom separation of 3 Å (4 Å) have also been calculated, as shown in Fig. 5. At a tip-adatom separation of 3 Å, in the $\text{Cu}(001)$ system, for the AP configuration, the spin-up transmission coefficient at E_F is only slightly smaller than that of the spin down, in contrast to those in the P configuration. A similar situation is also observed for the Cu_2N system in the P configuration. Since each of these two systems has different transmissions for the P and AP configurations, a large magnetoresistance ratio can be expected. The zero-bias magnetoresistance ratio is defined as $R_{\text{MR}} = (T_P - T_{\text{AP}})/T_{\text{AP}}$, with T_P (T_{AP}) being the transmission at E_F for the P (AP) configuration. We obtain $R_{\text{MR}} = 133\%$

(155%) for the Cu(001) system and $R_{MR} = 102\%$ (78%) for the $\text{Cu}_2\text{N}/\text{Cu}(001)$ system at a tip-adatom distance of 3 \AA (4 \AA).

Finally, it is worth noting that the antiferromagnetic exchange interaction between the Fe adatom and the Fe tip could lead to the formation of a singlet state [28]; that is, atoms could be entangled. Thus, our results suggest that for the junction on $\text{Cu}_2\text{N}/\text{Cu}(001)$, entanglement could exist for a large range of the tip-adatom separation due to the strong antiferromagnetic coupling, while on Cu(001) it could be possible to switch the entanglement on and off by changing the tip-adatom separation. The entanglement temperature T_e [47,59,60] (proportional to the exchange interaction) could be quite high in the Fe-Fe junctions.

IV. CONCLUSION

In conclusion, our results have demonstrated that the interactions between the adatom and the substrate have significant effects on the exchange interactions between the Fe tip and the

Fe adatom. An antiferromagnetic-ferromagnetic transition and antiferromagnetic exchange interactions between the tip and the adatom in junctions on Cu(001) and $\text{Cu}_2\text{N}/\text{Cu}(001)$ were revealed, respectively. The physics behind these phenomena is related to the competition between the coupling of the adatom with the substrate and the coupling of the tip with the adatom. Spin-dependent transmission properties have been calculated. We found large differences in spin polarization and magnetoresistance for junctions on the Cu(001) and $\text{Cu}_2\text{N}/\text{Cu}(001)$ surfaces.

ACKNOWLEDGMENTS

This work was supported by the National Natural Science Foundation of China (Grants No. NSFC-11274146, No. 11674143, No. 11474103, and No. 11474138); the Program for Changjiang Scholars and Innovative Research Team in University, Grant No. IRT-16R35; the Fundamental Research Funds for the Central Universities.

-
- [1] A. A. Khajetoorians, J. Wiebe, B. Chilian, S. Lounis, S. Blügel, and R. Wiesendanger, *Nat. Phys.* **8**, 497 (2012).
 - [2] F. Meier, L. H. Zhou, J. Wiebe, and R. Wiesendanger, *Science* **320**, 82 (2008).
 - [3] L. H. Zhou, J. Wiebe, S. Lounis, E. Vedmedenko, F. Meier, S. Blügel, P. H. Dederichs, and R. Wiesendanger, *Nat. Phys.* **6**, 187 (2010).
 - [4] N. Tsukahara, S. Shiraki, S. Itou, N. Ohta, N. Takagi, and M. Kawai, *Phys. Rev. Lett.* **106**, 187201 (2011).
 - [5] H. B. Heersche, Z. de Groot, J. A. Folk, L. P. Kouwenhoven, H. S. J. van der Zant, A. A. Houck, J. Labaziewicz, and I. L. Chuang, *Phys. Rev. Lett.* **96**, 017205 (2006).
 - [6] H. Prüser, P. E. Dargel, M. Bouhassoune, R. G. Ulbrich, T. Pruschke, S. Lounis, and M. Wenderoth, *Nat. Commun.* **5**, 5417 (2014).
 - [7] C. F. Hirjibehedin, C. P. Lutz, and A. J. Heinrich, *Science* **312**, 1021 (2006).
 - [8] A. A. Khajetoorians, J. Wiebe, B. Chilian, and R. Wiesendanger, *Science* **332**, 1062 (2011).
 - [9] B. Bryant, A. Spinelli, J. J. T. Wagenaar, M. Gerrits, and A. F. Otte, *Phys. Rev. Lett.* **111**, 127203 (2013).
 - [10] J. C. Oberg, M. R. Calvo, F. Delgado, M. Moro-Lagares, D. Serrate, D. Jacob, J. Fernandez-Rossier, and C. F. Hirjibehedin, *Nat. Nanotechnol.* **9**, 64 (2013).
 - [11] P. Ruiz-Díaz, O. V. Stepanyuk, and V. S. Stepanyuk, *J. Phys. Chem. C* **119**, 26237 (2015).
 - [12] N. Néel, J. Kröger, L. Limot, K. Palotas, W. A. Hofer, and R. Berndt, *Phys. Rev. Lett.* **98**, 016801 (2007).
 - [13] P. Wahl, P. Simon, L. Diekhöner, V. S. Stepanyuk, P. Bruno, M. A. Schneider, and K. Kern, *Phys. Rev. Lett.* **98**, 056601 (2007).
 - [14] A. F. Otte, M. Ternes, S. Loth, C. P. Lutz, C. F. Hirjibehedin, and A. J. Heinrich, *Phys. Rev. Lett.* **103**, 107203 (2009).
 - [15] A. Spinelli, M. Gerrits, R. Toskovic, B. Bryant, M. Ternes, and A. F. Otte, *Nat. Commun.* **6**, 10046 (2015).
 - [16] D. J. Choi, R. Robles, S. C. Yan, J. A. J. Burgess, S. R. Pissarczyk, J. P. Gauyacq, N. Lorente, M. Ternes, and S. Loth, *Nano Lett.* **17**, 6203 (2017).
 - [17] X. Qian and W. Hübner, *Phys. Rev. B* **67**, 184414 (2003).
 - [18] Y. Mokrousov, G. Bihlmayer, S. Blügel, and S. Heinze, *Phys. Rev. B* **75**, 104413 (2007).
 - [19] S. Loth, S. Baumann, C. P. Lutz, D. M. Eigler, and A. J. Heinrich, *Science* **335**, 196 (2012).
 - [20] H. X. Li, M. Huang, and C. Y. Cao, *J. Mater. Chem. C* **5**, 4557 (2017).
 - [21] L. Juárez-Reyes, G. M. Pastor, and V. S. Stepanyuk, *Phys. Rev. B* **86**, 235436 (2012).
 - [22] N. N. Negulyaev, V. S. Stepanyuk, W. Hergert, and J. Kirschner, *Phys. Rev. Lett.* **106**, 037202 (2011).
 - [23] R. Schmidt, C. Lazo, U. Kaiser, A. Schwarz, S. Heinze, and R. Wiesendanger, *Phys. Rev. Lett.* **106**, 257202 (2011).
 - [24] C. Lazo, V. Caciuc, H. Hölscher, and S. Heinze, *Phys. Rev. B* **78**, 214416 (2008).
 - [25] N. Hauptmann, J. W. Gerritsen, D. Wegner, and A. A. Khajetoorians, *Nano Lett.* **17**, 5660 (2017).
 - [26] S. Yan, D.-J. Choi, J. A. J. Burgess, S. Rolf-Pissarczyk, and S. Loth, *Nat. Nanotechnol.* **10**, 40 (2014).
 - [27] K. Tao, V. S. Stepanyuk, W. Hergert, I. Rungger, S. Sanvito, and P. Bruno, *Phys. Rev. Lett.* **103**, 057202 (2009).
 - [28] J. Bork, Y. H. Zhang, L. Diekhöner, L. Borda, P. Simon, J. Kroha, P. Wahl, and K. Kern, *Nat. Phys.* **7**, 901 (2011).
 - [29] N. Néel, J. Kröger, and R. Berndt, *Phys. Rev. B* **82**, 233401 (2010).
 - [30] D.-J. Choi, M. V. Rastei, P. Simon, and L. Limot, *Phys. Rev. Lett.* **108**, 266803 (2012).
 - [31] K. von Bergmann, M. Ternes, S. Loth, C. P. Lutz, and A. J. Heinrich, *Phys. Rev. Lett.* **114**, 076601 (2015).
 - [32] D. J. Choi, S. Guissart, M. Ormaza, N. Bachellier, O. Bengone, P. Simon, and L. Limot, *Nano Lett.* **16**, 6298 (2016).
 - [33] J. D. Ren, X. Wu, H. M. Guo, J. B. Pan, S. X. Du, H. G. Luo, and H. J. Gao, *Appl. Phys. Lett.* **107**, 071604 (2015).
 - [34] B. W. Heinrich, L. Braun, J. I. Pascual, and K. J. Franke, *Nano Lett.* **15**, 4024 (2015).
 - [35] Kun Tao, Q. Guo, P. Jena, D. S. Xue, and V. S. Stepanyuk, *Phys. Chem. Chem. Phys.* **17**, 26302 (2015).
 - [36] G. Kresse and J. Hafner, *Phys. Rev. B* **47**, 558 (1993).
 - [37] G. Kresse and J. Furthmüller, *Phys. Rev. B* **54**, 11169 (1996).

- [38] S. L. Dudarev, G. A. Botton, S. Y. Savrasov, C. J. Humphreys, and A. P. Sutton, *Phys. Rev. B* **57**, 1505 (1998).
- [39] At a tip-adatom separation of 3 Å, as $U = 2.0$ eV, the energy difference between the P and AP configurations E_{P-AP} is 258.56 meV, and it is 97.07 meV for $U = 5.0$ eV. For a separation of 4 Å, $E_{P-AP} = 80.65$ meV for $U = 2.0$ eV, and it is 33.18 meV for $U = 5.0$ eV.
- [40] We also checked our results for the Fe atom adsorbed on top of the Cu atom on the Cu(001) surface; our main results do not change.
- [41] C. F. Hirjibehedin, C.-Y. Lin, A. F. Otte, M. Ternes, C. P. Lutz, B. A. Jones, and A. J. Heinrich, *Science* **317**, 1199 (2007).
- [42] A. N. Rudenko, V. V. Mazurenko, V. I. Anisimov, and A. I. Lichtenstein, *Phys. Rev. B* **79**, 144418 (2009).
- [43] A. B. Shick, F. Máca, and A. I. Lichtenstein, *Phys. Rev. B* **79**, 172409 (2009).
- [44] C.-Y. Lin and B. A. Jones, *Phys. Rev. B* **83**, 014413 (2011).
- [45] J. W. Nicklas, A. Wadehra, and J. W. Wilkins, *J. Appl. Phys.* **110**, 123915 (2011).
- [46] M. C. Urdaniz, M. A. Barral, and A. M. Llois, *Phys. Rev. B* **86**, 245416 (2012).
- [47] D. I. Bazhanov, O. V. Stepanyuk, O. V. Farberovich, and V. S. Stepanyuk, *Phys. Rev. B* **93**, 035444 (2016).
- [48] W. A. Hofer, A. J. Fisher, R. A. Wolkow, and P. Grütter, *Phys. Rev. Lett.* **87**, 236104 (2001).
- [49] J. Taylor, H. Guo, and J. Wang, *Phys. Rev. B* **63**, 121104 (2001).
- [50] When the spin direction of the Fe adatom is set to be spin up, the majority parts of d states are fully occupied, while minority parts are only partially occupied. As the spin direction is flipped from spin up to spin down, the majority parts of d states become partially occupied, while the minority parts are fully occupied.
- [51] S. Loth, K. von Bergmann, M. Ternes, A. F. Otte, C. P. Lutz, and A. J. Heinrich, *Nat. Phys.* **6**, 340 (2010).
- [52] S. Alexander and P. W. Anderson, *Phys. Rev.* **133**, A1594 (1964).
- [53] A. Oswald, R. Zeller, P. J. Braspenning, and P. H. Dederichs, *J. Phys. F* **15**, 193 (1985).
- [54] J. B. Goodenough, *Phys. Rev.* **100**, 564 (1955).
- [55] J. B. Goodenough, *J. Phys. Chem. Solids* **6**, 287 (1958).
- [56] J. Kanamori, *J. Phys. Chem. Solids* **10**, 87 (1959).
- [57] G. Mándi and K. Palotás, *Appl. Surf. Sci.* **304**, 65 (2014).
- [58] P. Ferriani, C. Lazo, and S. Heinze, *Phys. Rev. B* **82**, 054411 (2010).
- [59] D. O. Soares-Pinto, A. M. Souza, R. S. Sarthour, I. S. Oliveira, M. S. Reis, P. Brandão, J. Rocha, and A. M. dos Santos, *Europhys. Lett.* **87**, 40008 (2009).
- [60] M. S. Reis, S. Soriano, A. M. dos Santos, B. C. Sales, D. O. Soares-Pinto, and P. Brandão, *Europhys. Lett.* **100**, 50001 (2012).